Brain Research 1841 (2024) 149128

Contents lists available at ScienceDirect

Brain Research

journal homepage: www.elsevier.com/locate/brainres

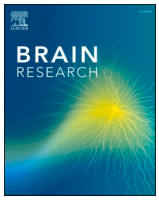

Research paper

Subthalamic nucleus deep brain stimulation induces functional deficits in norepinephrinergic neurotransmission in a Parkinson's disease model

Meike Statz [a], Hanna Weber [a], Frederike Weis [a], Maria Kober [a], Henning Bathel [b], Franz Plocksties [c], Ursula van Rienen [b,d,e], Dirk Timmermann [c], Alexander Storch [a,f], Mareike Fauser [a,*]

[a] Department of Neurology, University of Rostock, Gehlsheimer Straße 20, 18147 Rostock, Germany
[b] Institute of General Electrical Engineering, University of Rostock, 18059 Rostock, Germany
[c] Institute of Applied Microelectronics and Computer Engineering, University of Rostock, 18059 Rostock, Germany
[d] Department Life, Light and Matter, University of Rostock, 18059 Rostock, Germany
[e] Department of Ageing of Individuals and Society, Interdisciplinary Faculty, University of Rostock, 18059 Rostock, Germany
[f] German Centre for Neurodegenerative Diseases (DZNE) Rostock/Greifswald, Gehlsheimer Straße 20, 18147 Rostock, Germany

ARTICLE INFO

Keywords:
Deep brain stimulation
Subthalamic nucleus
6-Hydroxydopamine
Norepinephrine
Noradrenaline
Dopamine
Neurodegeneration

ABSTRACT

Background: Deep brain stimulation of the subthalamic nucleus (STN-DBS) is a successful treatment option in Parkinson's disease (PD) for different motor and non-motor symptoms, but has been linked to postoperative cognitive impairment.
Aim: Since both dopaminergic and norepinephrinergic neurotransmissions play important roles in symptom development, we analysed STN-DBS effects on dopamine and norepinephrine availability in different brain regions and morphological alterations of catecholaminergic neurons in the 6-hydroxydopamine PD rat model.
Methods: We applied one week of continuous unilateral STN-DBS or sham stimulation, respectively, in groups of healthy and 6-hydroxydopamine-lesioned rats to quantify dopamine and norepinephrine contents in the striatum, olfactory bulb and dentate gyrus. In addition, we analysed dopaminergic cell counts in the *substantia nigra pars compacta* and *area tegmentalis ventralis* and norepinephrinergic neurons in the *locus coeruleus* after one and six weeks of STN-DBS.
Results: In 6-hydroxydopamine-lesioned animals, one week of STN-DBS did not alter dopamine levels, while striatal norepinephrine levels were decreased. However, neither one nor six weeks of STN-DBS altered dopaminergic neuron numbers in the midbrain or norepinephrinergic neuron counts in the *locus coeruleus*. Dopaminergic fibre density in the dorsal and ventral striatum also remained unchanged after six weeks of STN-DBS. In healthy animals, one week of STN-DBS resulted in increased dopamine levels in the olfactory bulb and decreased contents in the dentate gyrus, but had no effects on norepinephrine availability.
Conclusions: STN-DBS modulates striatal norepinephrinergic neurotransmission in a PD rat model. Additional behavioural studies are required to investigate the functional impact of this finding.

1 Background

Deep brain stimulation of the subthalamic nucleus (STN-DBS) is a highly effective treatment option in middle- to late-stage Parkinson's disease (PD), offering both motor and non-motor symptom improvements to a varying degree (Funkiewiez et al., 2003, Deuschl et al., 2013,

Abbreviations: 6-OHDA, 6-hydroxydopamine; ACO, *commissura anterior*; AP, anterior-posterior; BW, body weight; DA, dopamine; DAB, diaminobenzidine; DV, dorsal–ventral; HPLC-ECD, high performance liquid chromatography with electrochemical detection; HRP, horseradish peroxidase; LC, *locus coeruleus*; MFB, median forebrain bundle; ML, medial–lateral; NACC, *nucleus accumbens*, core region; NE, noradrenaline/norepinephrine; OD, optical density; PD, Parkinson's disease; PDD, Parkinson's disease dementia; PD-MCI, mild cognitive impairment in Parkinson's disease; PFA, paraformaldehyde; SHAM, sham stimulation; SNpc, *substantia nigra pars compacta*; STIM, verum stimulation; STN-DBS, deep brain stimulation in subthalamic nucleus; STRd, dorsal striatum; TH, tyrosine hydroxylase; VTA, *area tegmentalis ventralis*.

* Corresponding author.
E-mail address: mareike.fauser@med.uni-rostock.de (M. Fauser).

https://doi.org/10.1016/j.brainres.2024.149128
Received 17 March 2024; Received in revised form 17 July 2024; Accepted 19 July 2024
Available online 23 July 2024

Dafsari et al., 2016, Dafsari et al., 2018). However, STN-DBS treatment can be associated with different side effects, some of which depend on the spreading of the electric fields into adjacent structures, resulting e.g. in dysarthria (Volkmann et al., 2002).

Degeneration of norepinephrinergic (NEergic) neurons in the *locus coeruleus* (LC) and associated reduction of norepinephrine (NE) levels is also a key feature of PD and has been linked to the development of various non-motor symptoms such as cognitive impairment, depression and apathy (Zweig et al., 1993, Pavese et al., 2011, Paredes-Rodriguez et al., 2020, Holland et al., 2021, Hezemans et al., 2022, Laurencin et al., 2023). However, the available literature provides only meagre data on the effects of NE enhancements on these symptoms in PD (Marsh et al., 2009).

In PD animal models, particularly in the 6-hydroxydopamine (6-OHDA) hemiparkinsonian model, neurorestorative effects of STN-DBS on dopaminergic (DAergic) neurons in the ventral midbrain have been demonstrated repeatedly (Temel et al., 2006, Spieles-Engemann et al., 2010, Fauser et al., 2021). However, STN-DBS effects on NEergic neurons in the *locus coeruleus* and NEergic neurotransmission have not been assessed so far.

In the present study, we investigate the influence of continuous STN-DBS on dopamine (DA) and NE (hereafter referred to as catecholamines) availability in the hippocampus, striatum and olfactory bulb as well as DAergic and NEergic neuron counts in respective mid- and hindbrain regions in the unilateral 6-OHDA rat model of PD and in healthy control rats. Since neurorestorative influences on a cellular level might be subjected to longer time constants than effects on neurotransmitter availability, we assessed catecholaminergic neuron counts after both one and six weeks of continuous STN-DBS. We hypothesize that STN-DBS – in addition to its influences on the DAergic system – also alters NEergic pathways.

2. Methods

Animals. All procedures were approved by responsible authorities (Landesdirektion Sachsen, Germany and Landesamt für Landwirtschaft, Lebensmittelsicherheit und Fischerei Mecklenburg-Vorpommern; reference numbers 7221.3-1-051/17, 7221.3-1-075/18 and 7221.3-1-011/21) and carried out in line with ARRIVE guidelines and the EU Directive 2010/63/EU. We used three cohorts of male Wistar rats (~240–260 g at purchase, Charles River Laboratories, Sulzfeld, Germany) that were kept under a 12 h/12 h light–dark cycle and had *ad libitum* access to food and water. In detail, cohort 1 consists of nine healthy control and seven 6-OHDA-lesioned animals with sham stimulation ($CTRL_{SHAM}$, $6\text{-}OHDA_{SHAM}$) as well as four and ten animals with short-term STN-DBS ($CTRL_{STIM}$, $6\text{-}OHDA_{STIM}$) respectively, whereas in cohort 2 only $6\text{-}OHDA_{SHAM}$ ($n = 6$) and $6\text{-}OHDA_{STIM}$ ($n = 8$) animals were used. In cohort 3, there were five unstimulated control animals as well as seven 6-OHDA animals with sham stimulation and six with long-term STN-DBS. Within the different cohorts, we excluded three animals in cohort 1 (one due to insufficient 6-OHDA lesioning defined as $\leq$3 rpm and two due to DBS failures), four animals in cohort 2 (two due to insufficient lesioning and two due to DBS failures) and two animals in cohort 3 (one due to insufficient lesioning, one due to DBS failure). Rats were first housed two per cage until electrode implantation, then they were housed one per cage to prevent reciprocal electrode and stimulator destruction (cohorts 1/2, equipped with external stimulators (Badstuebner et al., 2017)) or pair-housed during the entire study (cohort 3, equipped with fully implantable neurostimulators (Plocksties et al., 2021)).

For 6-OHDA lesioning, rats were anesthetized with isoflurane (5 % in 0.8 l O_2/min for 1 min, followed by 2–2.5 % during procedures) and additional weight-adapted ketamine/xylazine administration (1.4 ml/kg bodyweight (BW) of 25 mg/ml ketamine (Pfizer, Germany) and 20 mg/ml xylazine (Rompun, Bayer Healthcare, Germany). Animals then underwent right-sided 6-OHDA lesioning (6 mg/ml in 0.9 % NaCl with 0.2 mg/ml ascorbic acid; Sigma-Aldrich, Taufkirchen, Germany) to generate a reliable DAergic degeneration in the ventral midbrain as described previously in detail (Fauser et al., 2021, Statz et al., 2023): rats were placed in a stereotaxic frame (Stoelting Neuroscience, Dublin, Ireland) and 6-OHDA was injected at a flow rate of 1 µl/min via a 5 µL Hamilton syringe into the right median forebrain bundle (MFB) at the following coordinates: 4 µl at anterior-posterior (AP) −2.3; medial–lateral (ML) −1.5; dorsal–ventral (DV) −9.0 from bregma and dura, respectively, according to the rat brain atlas (Paxinos and Watson, 2007). Successful phenotype induction was quantified by apomorphine-induced rotational behaviour (0.25 mg/kg BW apomorphine, Teclapharm, Lüneburg, Germany; >3 rpm over 30 min) four to six weeks after lesioning (for details on experimental design, see Fig. 1). Healthy animals received sham injections with 0.9 % saline. For analgesia, we administered metamizole orally via drinking water for seven days perioperatively (1 g/1; Ratiopharm, Germany). Studies in all three cohorts were conducted independently; within the respective studies, all animals were divided into closely matched groups according to the quantitative results from apomorphine rotational testing: in cohort 1, $6\text{-}OHDA_{SHAM}$ animals showed average rotations of 6.5 ± 1.3 turns/min in contrast to $6\text{-}OHDA_{STIM}$ animals with 8.2 ± 1.0 turns/min ($P = 0.32$; from Welch's *t* test), while in cohort 3, animals displayed 7.3 ± 0.5 turns/min in $6\text{-}OHDA_{SHAM}$ rats and 6.7 ± 0.4 turns/min in $6\text{-}OHDA_{STIM}$ animals ($P = 0.48$; from unpaired two-sided *t* test). Rotational testing from cohort 2 has already been published in (Helf et al., 2023). Health surveillance was carried out daily by experienced raters and included daily weight measurement and rating of general appearances with predefined humane endpoints.

DBS Surgery. For investigation of functional changes of neurotransmitter levels, we used seven days of continuous STN-DBS (cohort 1), while for assessment of morphological changes in the DAergic and NEergic systems, we used animals with both one week of STN-DBS (cohort 2, tissue taken from a previous cohort with similar treatments as published in (Helf et al., 2023)) and an additional long-term STN-DBS cohort, which was treated for six weeks (cohort 3). In all animals, we used self-developed neurostimulators as detailed in (Plocksties et al., 2021); in cohorts 1 and 2, neurostimulators were covered in Velcro pouches and carried in a rodent backpack (total weight incl. backpack ~10 g), while for long-term DBS of six weeks (cohort 3), we used fully implanted stimulators encapsulated in 3D-printed polyethylen terephthalate (PETG) covers (Smart Materials 3D, Jaen, Spain) filled with epoxy resin (EP 601, Polytec PT, Karlsbad, Germany) and coated with biocompatible silicone (Nusil MED 10-667, Avantor, Center Valley, PA, US; total weight ~5 g). Since the rodent backpack to some extent impaired mobility of the animals compared to fully implanted devices, we used the latter as soon as they became available for animal welfare reasons. We implanted custom-made unipolar, rounded platinum-iridium electrodes (Microprobes for Life Sciences, MD, US) into the right STN of both healthy and 6-OHDA-lesioned animals. For the one-week DBS study in cohorts 1 and 2, rats were left to recover for seven days after electrode implantations until DBS onset or sham stimulation. We used the following stimulation parameters: 100 µA, 130 Hz, 60 µs with passive charge balancing. The stimulators allowed daily function control via a magnetically triggered built-in self-test resulting in specific blinking patterns (as detailed in (Plocksties et al., 2021)), which was visible through the backpack and could therefore be carried out in freely-moving animals within their home cages. After one week of stimulation, all animals were anesthetized and transcardially perfused with heparinized 0.9 % saline (20 I.E. heparin/ml) for 5 min, followed by ice-cold 0.9 % NaCl for 20 min (adapted from (Spieles-Engemann et al., 2011)). Brains were harvested, snap-frozen and stored at −80 °C until further processing. For ancillary analyses of effects of STN-DBS on NEergic neuron counts within the LC after one week of stimulation, we used paraformaldehyde-fixed tissue with similar experimental paradigms (cohort 2; results of dopaminergic cell counts and dopaminergic fibre densities already published in (Helf et al., 2023)).

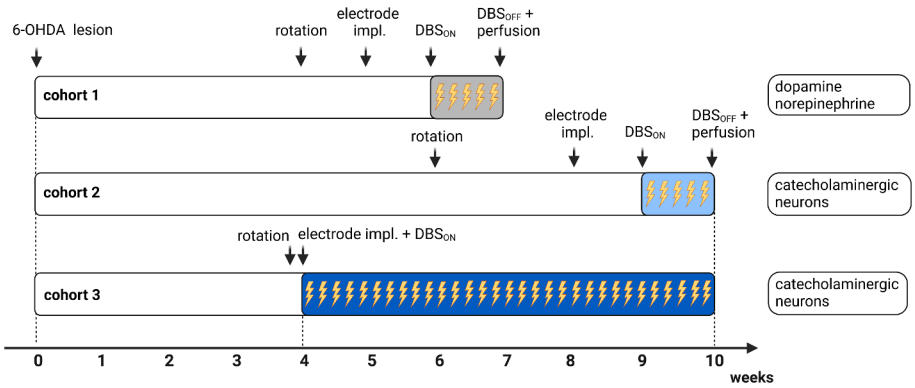

Fig. 1. Experimental design In all three cohorts, rats received unilateral injections of 6-OHDA into the right MFB and were submitted to apomorphine-induced rotational testing four to six weeks later. Experimental groups of 6-OHDA-lesioned animals were balanced according to their rotational behavior. All animals were implanted with DBS electrodes into the right STN. In cohorts 1 and 2, rats were left to recover for one week after electrode implantations until external neurostimulators (located in a rodent backpack) were switched on and STN-DBS was carried out for one week. Afterwards, brains were harvested for detection of catecholamine levels (cohort 1) or quantification of catecholaminergic neurons (cohort 2); results from dopaminergic neuron counts in cohort 2 have already been published in (Helf et al., 2023). In cohort 3, neurostimulators were fully implanted during the same procedure as electrode implantations and switched on the day after for continuous STN-DBS for six weeks. Stimulation was then discontinued and brains harvested for histological quantifications of catecholaminergic neurons and striatal dopaminergic fibre density. Abbreviations: 6-OHDA – 6-hydroxydopamine; MFB – median forebrain bundle; STN – subthalamic nucleus; DBS – deep brain stimulation; CTRL – control animals; SHAM – sham stimulation. Created with www.biorender.com.

In cohort 3, neurostimulators were implanted paravertebrally at the level of the interscapular line, wires were tunnelled along the neck and animals equipped with identical electrodes as in cohorts 1 and 2. DBS was switched on the day after surgery and continued for six weeks. Function control was carried out daily as described above with blinking patterns visible through the skin. Sham-stimulated and healthy animals, respectively, received identical treatments, including electrode implantations and dummy stimulators. At the end of the DBS period, stimulators were switched off and animals were transcardially perfused with 4 % paraformaldehyde (PFA). Brains were harvested, dehydrated in 30 % sucrose for 48 h and snap-frozen.

Microdissections. Saline-perfused brains from cohort 1 were transferred to −20 °C for 45 min, inserted into a metal brain matrix (Stoelting Neuroscience, Dublin, Ireland) and manually cut into ~0.5–1 mm thick sections, which were stored on a cooling plate (cop 30, Medite Medical, Burgdorf, Germany). Before the dissection of specific brain areas, respective midbrain sections were inspected under a microscope for correct electrode placement. The following brain regions as identified from the rat brain atlas (Paxinos and Watson, 2007) were dissected using the Palkovits Punch technique with a 1 mm tissue punch or fine scissors, as appropriate (both from Stoelting Neuroscience, Dublin, Ireland): medial part of the striatum (similar to our previous study (Weselek et al., 2020); the lateral part does not receive a relevant norepinephrinergic input (Nomura et al., 2014)), olfactory bulb and dentate gyrus of the hippocampus. Since we used a unilateral 6-OHDA model (due to a significant risk of severe adverse effects, e.g. dysphagia, in bilaterally lesioned animals), all regions were separately dissected from the right (lesioned, if applicable; ipsilateral) and left (non-lesioned; contralateral) hemispheres. Tissue samples were placed in 300 µl RIPA buffer (Pierce ™) with 1:9 protease inhibitor 100x (Halt™, both Thermo Fisher Scientific, MA, US), homogenised (Precellys 24 Dual Tissue Homogenizer, Bertin Technologies, France), incubated on ice, centrifuged at 14,000 rpm for 3 min and stored at −20 °C until further processing (adapted from (Spieles-Engemann et al., 2011)).

DA and NE assays. For DA and NE quantifications in cohort 1, we used commercially available ELISA kits with streptavidin–biotin detection (RayBiotech Life, GA, US) with detection limits of 4 pg/ml for DA and 20 pg/ml for NE. Sample input was adjusted to total protein concentrations in the respective samples according to manufacturer's protocol. For all samples and standards, duplicate assays were conducted. ELISAs were performed according to the manufacturer's protocol: samples and standards were applied to the 96-well plate coated with the capture antibody and incubated for 2.5 h with gentle shaking. After washing four times with the kit's wash buffer, detection antibodies were added, incubated for 1 h, washed four times and incubated with HRP-conjugated streptavidin for 45 min. After additional four washing steps, 3,3,5,5′-tetramethylbenzidine substrate solution was added, incubated for 30 min in the dark and stopped with sulphuric acid, resulting in a colour change to yellow. The colour intensity was read photometrically at 405 nm (Spark Multimode Microplate Reader, Tecan, Germany) and converted to DA or NE concentrations by power regression of the standard series.

Protein assays were carried out with a ready-to-use kit (Pierce™ BCA Protein Assay, Thermo Fisher Scientific, MA, US) using 10 µl of each standard or sample diluted in 200 µl working reagent of the kit in a 96-well plate. Measured absorbances were calculated by linear regression of the standard series (range 0.125 µg/µl to 2 µg/µl) to total protein. DA and NE amounts were normalized to total protein concentration of the respective sample.

Immunohistochemistry. For DAB immunostaining of TH^+ catecholaminergic neurons and striatal DAergic fibre density in cohort 2 and 3, brains were sectioned on a cryotome, while accuracy of electrode placement was visually inspected during tissue sectioning. 30 µm free-floating coronal sections from PFA-fixed brains were processed as described earlier (Brandt et al., 2017) with mouse anti-TH antibody (1:1000; RRID: AB_477560; Sigma Aldrich, Taufkirchen, Germany) and a commercially available ABC Elite Kit (Vector Laboratories, US) containing the biotinylated secondary antibody, ABC and 3, 3́-diaminobenzidine (DAB) solutions according to manufactureŕs instructions.

Imaging and quantification. For catecholaminergic cell counts in cohorts 2 and 3, catecholaminergic TH^+ neurons were imaged and quantified throughout the entire *substantia nigra pars compacta* (SNpc), the *area tegmentalis ventralis* (VTA) and the *locus coeruleus* (LC) using a motorized Axio.Observer.Z1 and ZEN Blue 2.3 software with Tiles and Position Module and in-built Image Analysis Module (all Carl Zeiss, Oberkochen, Germany). To assess DAergic fibre density, we quantified optical densities (OD) in the dorsal striatum (STRd) and the ventral striatum, i.e. the core region of the *nucleus accumbens* (NACC), with the *commissura anterior* (ACO) as a reference region as detailed in (Fauser et al., 2021). TH^+ fibre densities were calculated as follows: $-1 \times (OD_{STRd} - OD_{ACO})$ and $-1 \times (OD_{NACC} - OD_{ACO})$.

Statistics. Analyses, data plots and figures were carried out with GraphPadPrism 9.4.1 (GraphPad Software, CA, US) and BioRender.com

(BioRender, Canada). Shapiro-Wilk test and visual inspection of box plots were applied to test for normal distribution. Homogeneity of variances was analysed with Levene's test. We used Students unpaired two-sided *t*-test or mixed ANOVA with Fischer LSD *post-hoc* analysis to determine mean differences between groups, as appropriate. DA and NE levels below detection levels were generated with the random number generator in Excel (Microsoft, WA, US) between zero and the lower detection limit. All data are presented as mean ± standard error of the mean (S.E.M.). Statistical significance was set at $P < 0.05$.

3. Results

In the present study, we analysed effects of STN-DBS on functional and morphological integrity of the DAergic and NEergic systems in the unilateral 6-OHDA-induced model of PD and in healthy control rats. In previous studies, we already demonstrated an increase in DAergic neuron counts and striatal DAergic fibre density after long-term bilateral STN-DBS of six weeks, though without data on the NEergic system (Badstuebner et al., 2017, Fauser et al., 2021, Helf et al., 2023).

3.1. STN-DBS reduces striatal norepinephrine levels after 6-OHDA lesioning

We assessed DA and NE levels in different target regions, i.e. the striatum, the olfactory bulb and the dentate gyrus of the hippocampus in 6-OHDA-lesioned rats (6-OHDA$_{SHAM}$: n = 6; 6-OHDA$_{STIM}$: n = 8) and healthy controls (CTRL$_{SHAM}$: n = 9; CTRL$_{STIM}$: n = 4; cohort 1) after one week of STN-DBS.

In 6-OHDA$_{SHAM}$ rats, DA levels in the olfactory bulb were 1.2 ± 0.1 ng/mg protein in contralateral (non-lesioned) hemispheres and 0.8 ± 0.1 ng/mg protein on the ipsilateral (lesioned) sides (F(1,10) = 4.79; $P = 0.002$), while in 6-OHDA$_{STIM}$ animals respective DA levels were 0.9 ± 0.1 ng/mg protein and 1.1 ± 0.1 ng/mg protein (Fig. 2**a**, upper panel). Mixed ANOVA revealed a significant interaction effect between lesioned/non-lesioned hemispheres and short-term STN-DBS (F(1,10) = 19.97; $P = 0.001$), but no main effect of either hemisphere (F(1,10) = 4.79; $P = 0.05$) or short-term STN-DBS (F(1,11) = 0.0005; $P = 0.98$). In the striatum, DA levels in contralateral hemispheres were 65.1 ± 15.4 ng/mg protein in comparison to 0.8 ± 0.1 ng/mg protein in ipsilateral sides in 6-OHDA$_{SHAM}$ animals, while 6-OHDA$_{STIM}$ animals displayed 80.4 ± 19.4 ng/mg protein and 0.4 ± 0.1 ng/mg protein, respectively (Fig. 2**a**, middle panel). There was no significant interaction effect between hemispheres and short-term STN-DBS (F(1,23) = 0.34; $P = 0.57$),

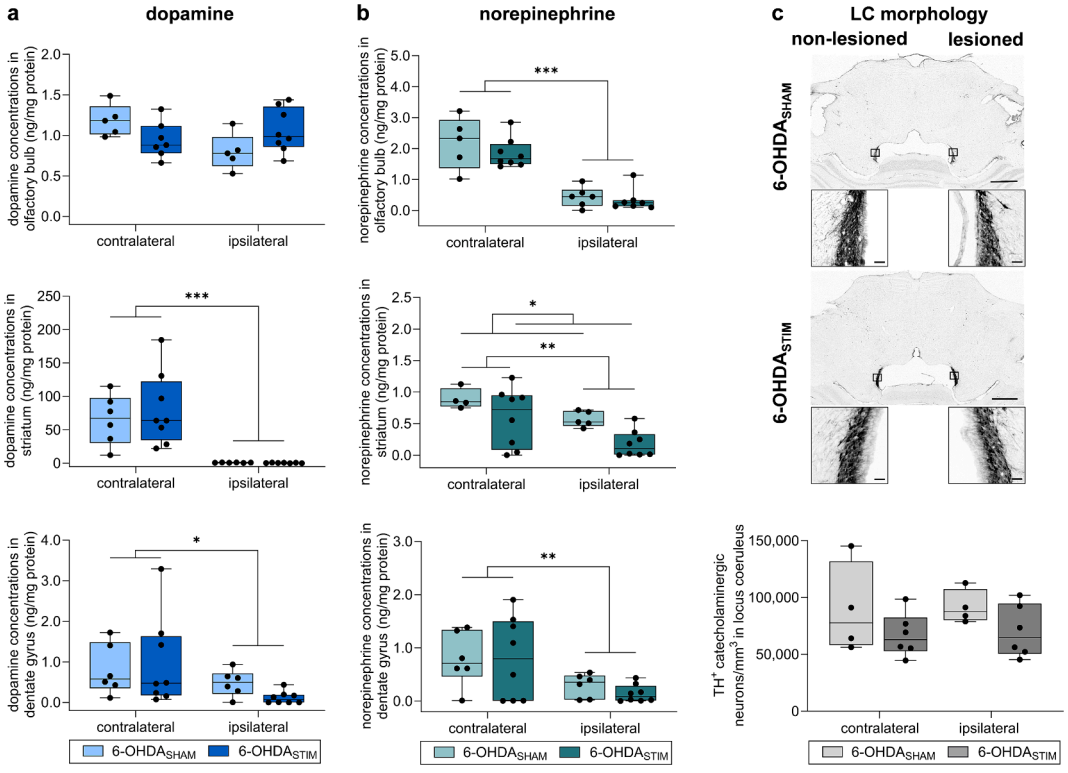

Fig. 2. Alterations in dopaminergic and norepinephrinergic neurotransmission induced by subthalamic nucleus deep brain stimulation (STN-DBS) in unilaterally 6-OHDA-lesioned rats (a) Regarding dopamine levels in the olfactory bulb (upper panel), there was a significant interaction effect $_{\text{hemispheres x short-term STN-DBS}}$ (F(1,10) = 19.97; $P = 0.001$), while in the striatum (middle panel), we found a significant main effect of 6-OHDA lesion on dopamine levels (F(1,23) = 28.33; $P < 0.0001$), but no main effect of short-term stimulation. Similarly, in the dentate gyrus of the hippocampus (lower panel), there was a main effect of 6-OHDA lesion (F(1,12) = 0.12; $P = 0.04$) on dopamine levels but no main effect of STN-DBS. **(b)** Regarding norepinephrine levels in the olfactory bulb (upper panel), we found a main effect of 6-OHDA lesion (F(1,10) = 137.6; $P < 0.0001$) without a significant main effect of short-term STN-DBS. In the striatum (middle panel), there were main effects of both 6-OHDA lesion (F(1,10) = 15.99; $P = 0.003$) and STN-DBS (F(1,11) = 5.33; $P = 0.04$). In the dentate gyrus of the hippocampus (lower panel), we found a main effect of 6-OHDA lesion (F(1,12) = 13.49; $P = 0.003$), without an additional main effect of STN-DBS. **(c)** Representative immunohistological images of TH staining in the LC of hemiparkinsonian rats with either sham stimulation (6-OHDA$_{SHAM}$, upper panel) or unilateral, right-sided STN-DBS for one week (6-OHDA$_{STIM}$, middle panel; cohort 2). Scale bars, 1000 μm and 50 μm. Quantitative analysis of TH$^+$ norepinephrinergic neurons in the LC in 6-OHDA$_{SHAM}$ and 6-OHDA$_{STIM}$ animals showed no effects of 6-OHDA-lesioning or short-term STN-DBS (lower panel). Data on dopaminergic cell counts in this cohort have already been published in (Helf et al., 2023), again with no effect of STN-DBS on dopaminergic cell counts in the SNpc and VTA or on dopaminergic fibre density in the striatum. *P*-values are from mixed ANOVA with Fisher LSD *post-hoc* analysis. Main effects are shown with overarching brackets, while interaction effects are only mentioned in the caption for clarity. Abbreviations: 6-OHDA – 6-hydroxydopamine; SHAM – sham stimulation; STIM – verum stimulation.

however a main effect of the lesion ($F(1,23) = 28.33$; $P < 0.0001$), but no main effect of short-term STN-DBS ($F(1,23) = 0.30$; $P = 0.59$). In the dentate gyrus of the hippocampus, we found DA levels of 0.8 ± 0.3 ng/mg protein and 0.5 ± 0.1 ng/mg protein in contralateral and ipsilateral hemispheres in 6-$OHDA_{SHAM}$ rats and 1.0 ± 0.4 vs. 0.1 ± 0.1 ng/mg protein in 6-$OHDA_{STIM}$ animals (Fig. 2**a**, lower panel). There was no significant interaction effect between hemispheres and short-term STN-DBS ($F(1,12) = 1.12$; $P = 0.31$) and no main effect of short-term stimulation ($F(1,12) = 0.12$; $P = 0.74$), but a significant main effect of the lesion ($F(1,12) = 5.56$; $P = 0.04$). In healthy animals, there was no significant interaction effect between hemispheres, i.e. electrode placement, and stimulation in any of the examined regions, but a main effect of short-term stimulation in the olfactory bulb and dentate gyrus (see Suppl. **Fig. S1b** and **Suppl. Table S1** for statistical results).

Regarding NE levels in the olfactory bulb, we found 2.2 ± 0.4 ng/mg protein and 0.4 ± 0.1 ng/mg protein in contralateral and ipsilateral hemispheres in 6-$OHDA_{SHAM}$ animals and 1.9 ± 0.2 ng/mg protein and 0.3 ± 0.1 ng/mg protein in 6-$OHDA_{STIM}$ animals (Fig. 2**b**, upper panel). There was no significant interaction effect between hemispheres and short-term STN-DBS ($F(1,10) = 0.44$; $P = 0.52$) and no main effect of short-term stimulation ($F(1,12) = 0.63$; $P = 0.44$), but a significant main effect of the lesion ($F(1,10) = 137.6$; both $P < 0.0001$). In the striatum, NE levels were 0.9 ± 0.1 ng/mg protein and 0.6 ± 0.1 ng/mg protein in contralateral and ipsilateral hemispheres, while in 6-$OHDA_{STIM}$ animals NE levels were 0.6 ± 0.2 ng/mg protein and 0.2 ± 0.1 ng/mg protein (Fig. 2**b**, middle panel). Mixed ANOVA revealed no significant interaction effect between lesioned/non-lesioned hemispheres and STN-DBS ($F(1,10) = 0.19$; $P = 0.67$), but a significant main effect of both short-term stimulation ($F(1,11) = 5.33$; $P = 0.04$) and lesion ($F(1,10) = 15.99$; $P = 0.003$). In the dentate gyrus of the hippocampus, NE levels were 0.8 ± 0.2 ng/mg protein and 0.3 ± 0.1 ng/mg protein in contralateral and ipsilateral hemispheres in 6-$OHDA_{SHAM}$ animals, while 6-$OHDA_{STIM}$ animals displayed 0.8 ± 0.3 ng/mg protein and 0.1 ± 0.1 ng/mg protein respectively (Fig. 2**b**, lower panel). Again there was no interaction effect between hemispheres and short-term STN-DBS ($F(1,1) = 0.28$; $P = 0.61$) and no main effect of short-term STN-DBS ($F(1,12) = 0.10$; $P = 0.76$), but a significant main effect of the lesion ($F(1,12) = 13.49$; $P = 0.003$). We found no interaction effect and no main effects of electrode placement and short-term STN-DBS on NE levels in healthy control rats in any brain region (see **Suppl. Fig. S1b** and **Suppl. Table S2** for statistical results).

3.2. Chronic STN-DBS does not alter dopaminergic and norepinephrinergic cell counts and striatal fibre densities

Next, we were interested in whether the alterations in NE levels could be attributed to morphological alterations in the LC: first, we analysed total neuronal cell counts of TH^+ NEergic neurons after one week of continuous STN-DBS (cohort 2, 6-$OHDA_{SHAM}$: n = 6; 6-$OHDA_{STIM}$: n = 4; Fig. 2**c**). All data are presented as mean ± S.E.M.. Tissue for LC immunohistochemistry was taken from an already published cohort (Helf et al., 2023) without additional healthy control rats, which received similar treatments (cohort 2, Fig. 1). TH^+ NEergic cell counts in the LC were 89,238 ± 20,116 TH^+ neurons/mm^3 in the contralateral (non-lesioned, non-implanted) and 87,916 ± 8,857 TH^+ neurons/mm^3 in the ipsilateral (6-OHDA-lesioned, electrode-implanted) hemispheres in 6-$OHDA_{SHAM}$ animals, while in 6-$OHDA_{STIM}$ rats the cell counts were 66,991 ± 7,826 TH^+ neurons/mm^3 and 70,335 ± 9,399 TH^+ neurons/mm^3. There was no interaction effect between hemispheres and short-term STN-DBS ($F(1,8) = 0.16$; $P = 0.7$) and no main effect of either 6-OHDA lesion ($F(1,8) = 0.03$; $P = 0.87$) or short-term STN-DBS ($F(1,8) = 1.69$; $P = 0.23$; Fig. 2**c**). DAergic cell counts in the SNpc and VTA were also unchanged as already published in (Helf et al., 2023).

Since morphological effects on a cellular level might not be evident after a stimulation period of one week, we performed additional long-term STN-DBS over six weeks (cohort 3, $CTRL_{SHAM}$: n = 5; 6-$OHDA_{SHAM}$: n = 7; 6-$OHDA_{STIM}$: n = 6). Here, we analysed total neuronal cell counts of TH^+ DAergic neurons in the SNpc, VTA and TH^+ NEergic neurons in the LC.

Healthy animals displayed no alterations due to electrode placement between contralateral and ipsilateral hemispheres in the SNpc and VTA (see **Suppl.** Fig. S2**a**). In the SNpc, TH^+ DA cell counts in 6-$OHDA_{SHAM}$ rats were 15,266 ± 375 TH^+ neurons/mm^3 in the contralateral hemispheres vs. 286 ± 119 TH^+ neurons/mm^3 in ipsilateral sides, while in 6-$OHDA_{STIM}$ the cell counts were 18,271 ± 2,834 TH^+ neurons/mm^3 and 385 ± 92 TH^+ neurons/mm^3, respectively. There was a significant main effect of 6-OHDA lesioning ($F(1,19) = 119.3$; $P < 0.0001$), though no main effect of long-term STN-DBS ($F(1,19) = 1.06$; $P = 0.32$) and no interaction effect of hemispheres and long-term STN-DBS ($F(1,19) = 0.93$; $P = 0.35$; Fig. 3**b**). In the VTA, total DAergic neuron counts were 4,831 ± 1,597 TH^+ neurons/mm^3 in ipsilateral in comparison to 16,472 ± 4,022 TH^+ neurons/mm^3 in contralateral hemispheres in 6-$OHDA_{SHAM}$ animals and 2,142 ± 363 TH^+ neurons/mm^3 and 12,942 ± 2,226 TH^+ neurons/mm^3 in6-$OHDA_{STIM}$, respectively. Again, there was a significant main effect of the lesion ($F(1,10) = 33.73$; $P = 0.002$), but no main effect of long-term STN-DBS ($F(1,11) = 0.83$; $P = 0.38$) and no interaction effect between hemispheres and long-term STN-DBS ($F(1,10) = 0.09$; $P = 0.77$; Fig. 3**b**).

In the LC, there was no effect of 6-OHDA lesioning, as 6-$OHDA_{SHAM}$ animals displayed 41,733 ± 6,766 TH^+ neurons/mm^3 in contralateral in comparison to 42,197 ± 6,468 TH^+ neurons/mm^3 in ipsilateral hemispheres ($P = 0.88$), while in 6-$OHDA_{STIM}$ animals the NE cell count were 38,959 ± 1,008 TH^+ neurons/mm^3 in contralateral and 38,168 ± 3,967 TH^+ neurons/mm^3 in ipsilateral hemispheres ($F(1,10) = 0.15$; $P = 0.71$). Moreover there was no effect of long-term STN-DBS ($F(1,11) = 0.35$; $P = 0.57$) and no interaction effect between hemispheres and long-term STN-DBS ($F(1,10) = 0.035$; $P = 0.85$; Fig. 4**b**). A similar number of neurons was found in the LC of healthy animals (contralateral: 31,601 ± 4,437 TH^+ neurons/mm^3; ipsilateral: 29,695 ± 1,389 TH^+ neurons/mm^3), while electrode placement did not have any effect ($P = 0.72$; Fig. 4**d**). In addition to total neuron counts in the DAergic and NEergic regions, we assessed striatal DAergic fibre density in the dorsal (STRd) and ventral striatum (*nucleus accumbens* core region, NACC) with optical density (OD) measurements relative to a reference region (*commissura anterior*, ACO). In both areas, electrode placement did not affect DAergic fibre density in healthy animals (**Suppl. Fig. S2d**), while in the STRd, TH^+ fibre density was reduced due to 6-OHDA lesioning ($F(1,10) = 518.8$; $P < 0.0001$). As for TH^+ cell counts, there was no main effect of long-term STN-DBS ($F(1,10) = 0.1$; $P = 0.76$), but an interaction effect of hemispheres and long-term STN-DBS ($F(1,10) = 5.93$; $P = 0.04$). Similar effects were found in the NACC, where the TH^+ fibre density was reduced after 6-OHDA lesioning ($F(1,10) = 366.3$; $P < 0.0001$), while no main effect of long-term STN-DBS was found ($F(1,10) = 0.08$; $P = 0.78$), but an interaction effect between hemispheres and long-term STN-DBS ($F(1,10) = 12.48$; $P = 0.005$; Fig. 3**d**).

4. Discussion

The present study indicates that STN-DBS decreases striatal NE availability in the unilateral 6-OHDA rat model of PD, but not in healthy control animals. Since we did not detect any alterations of NEergic neuron counts within the LC after both 6-OHDA lesioning and STN-DBS, these effects cannot be attributed to changes in LC morphology in parkinsonian animals but seem to reflect functional changes in NEergic neurotransmission. In contrast, DAergic neurotransmission and neuron counts were not affected by one week of STN-DBS in the 6-OHDA rat model. Long-term STN-DBS over six weeks did also not affect catecholaminergic neuron counts and striatal fibre densities.

The understanding of the interplay between NEergic neurotransmission, STN function and DBS effects is of pivotal interest when trying to understand PD: the literature provides extensive evidence for a

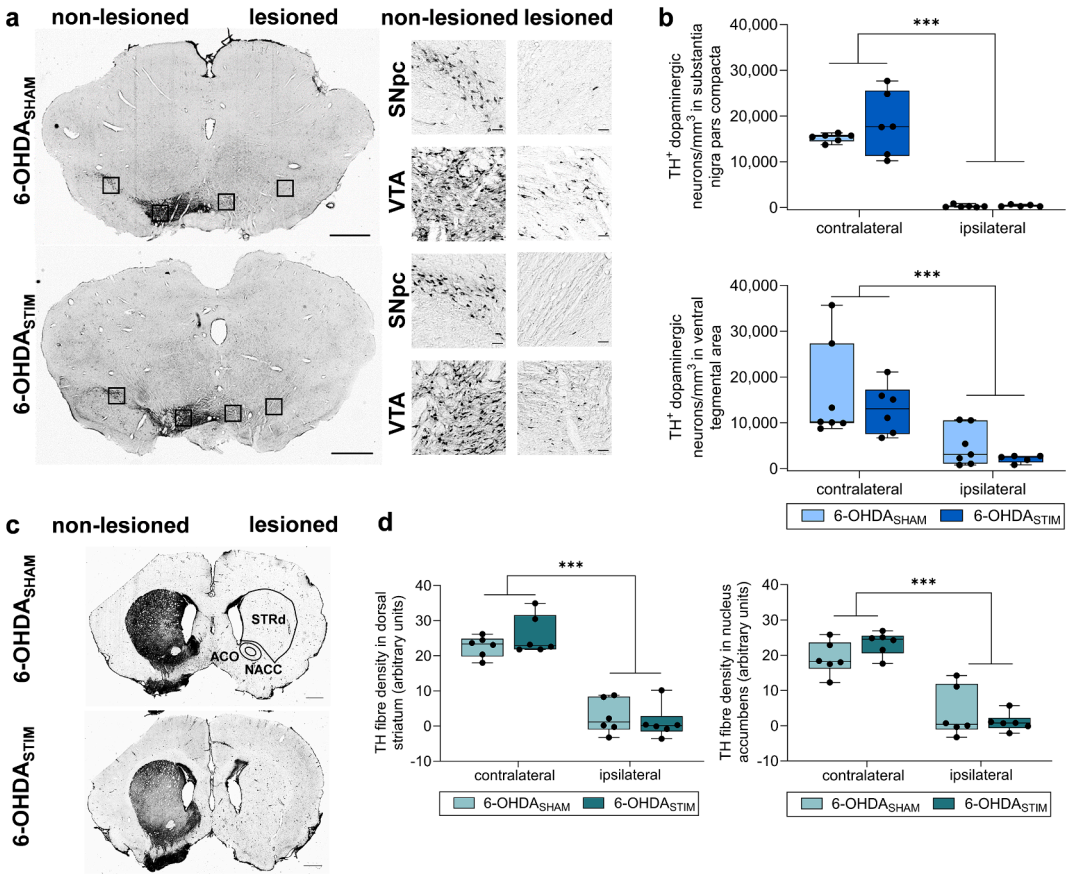

Fig. 3. Effects of six weeks of subthalamic nucleus deep brain stimulation (STN-DBS) on dopaminergic cell counts in unilaterally 6-OHDA-lesioned rats (a) Representative immunohistological images of tyrosine hydroxylase (TH) stainings in the *substantia nigra pars compacta* (SNpc) and *area tegmentalis ventralis* (VTA) of hemiparkinsonian rats with either unilateral, right-sided STN-DBS for six weeks (6-OHDA$_{STIM}$) or sham stimulation (6-OHDA$_{SHAM}$; cohort 3). Scale bars, 1000 μm and 50 μm. **(b)** Quantitative analysis of TH$^+$ dopaminergic neurons in the SNpc (upper panel) and VTA (lower panel) in 6-OHDA-lesioned animals with sham stimulation (6-OHDA$_{SHAM}$) or STN-DBS (6-OHDA$_{STIM}$). In the SNpc, there was a significant main effect of 6-OHDA lesion ($F(1,19) = 119.3$; $P < 0.0001$), but no main effect of long-term STN-DBS. Results in the VTA were similar with a significant main effect of 6-OHDA lesion ($F(1,10) = 33.73$; $P = 0.002$), but no main effect of STN-DBS after six weeks. **(c)** Representative immunohistological images of TH staining in the striatum of hemiparkinsonian rats with either unilateral, right-sided STN-DBS for six weeks (6-OHDA$_{STIM}$) or sham stimulation (6-OHDA$_{SHAM}$). We analysed optical densities in the dorsal striatum (STRd) and the *nucleus accumbens* core region (NACC) as the main target areas of midbrain dopaminergic fibres and the *commissura anterior* (ACO) as the reference region (white matter). Scale bars, 500 μm. **(d)** Densiometric analysis of TH$^+$ fibre densities revealed a main effect of 6-OHDA lesioning in both the STRd (left; $F(1,10) = 518.8$; $P < 0.0001$) and NACC (right; $F(1,10) = 366.3$; $P < 0.0001$) and an interaction effect of hemispheres x long-term STN-DBS ($F(1,10) = 5.93$; $P = 0.04$) and ($F(1,10) = 12.48$; $P = 0.005$). *P*-values are from mixed ANOVA with Fisher LSD *post-hoc* analysis. Main effects are shown with overarching brackets, while interaction effects are only mentioned in the caption for clarity. Abbreviations: STN – *nucleus subthalamicus*; DBS – deep brain stimulation; 6-OHDA – 6-hydroxydopamine; SHAM – sham stimulation; SNpc – *substantia nigra pars compacta*; VTA – *area tegmentalis ventralis*; STRd – dorsal striatum; NACC – *nucleus accumbens* core region; ACO – *commissura anterior*; LC – *locus coeruleus*.

relevant LC degeneration with subsequent disruption of NEergic neurotransmission in PD, which occurs to a similar extent and even prior to DAergic degeneration (Zarow et al., 2003, Ohtsuka et al., 2013, Betts et al., 2019, Madelung et al., 2022). Indeed, dysfunction of NEergic circuitries has been linked to non-motor dysfunction in PD, e.g. to depression and cognitive dysfunction (Delaville et al., 2011, Alosaimi et al., 2022, Krohn et al., 2023). On the structural level, significant NEergic projections from the LC to the STN have been described in rodents and non-human primates (Belujon et al., 2007, Schmitt and Eipert, 2012, Schmitt et al., 2016); however, clinical studies are not available to date (reviewed in (Emmi et al., 2023)). On the clinical level, pharmacological NE manipulation seems to impact PD symptom severity alongside STN-DBS (Coenen et al., 2008, Albares et al., 2015), while in the 6-OHDA model, complete catecholaminergic depletion, i.e. combined DAergic and NEergic depletion, reduces STN-DBS therapeutic efficiency (Faggiani et al., 2015).

In contrast to the above-mentioned study, we here used a 6-OHDA PD rat model without any cellular evidence of NEergic dysfunction pre-DBS to study the effects of STN-DBS on NEergic neurotransmission. Moreover, we did not specifically protect NEergic neurons from the acute toxicity of 6-OHDA with desipramine, a norepinephrine reuptake inhibitor. However, the reports on the effects of 6-OHDA lesioning (in the median forebrain bundle) on NE levels are controversial in the literature (Waddington, 1980, Wang et al., 2010, Guimarães et al., 2013, Ostock et al., 2014). In our model of completed DAergic degeneration, we showed – to the best of our knowledge for the first time – that STN-DBS decreases NE availability in the striatum and without evidence of NEergic neuron degeneration within the LC (after one and even six weeks of STN-DBS). The reasons why these effects are specific for the PD model and not observed in healthy control animals remain enigmatic and need further clarification.

Our analyses of the DAergic systems revealed the expected severe reduction in DAergic neuron counts in the SNpc and VTA as well as in dopaminergic terminals in the STRd and NACC, without evidence of any STN-DBS effects. These results are in contrast to our previous studies showing neurorestorative effects in the DAergic systems after six weeks of STN-DBS (Fauser et al., 2021). However, the present cohort received only *unilateral* DBS in contrast to *bilateral* stimulation in our previous study; furthermore, we used different neurostimulators (Ewing et al., 2013, Badstuebner et al., 2017) and also different stimulation

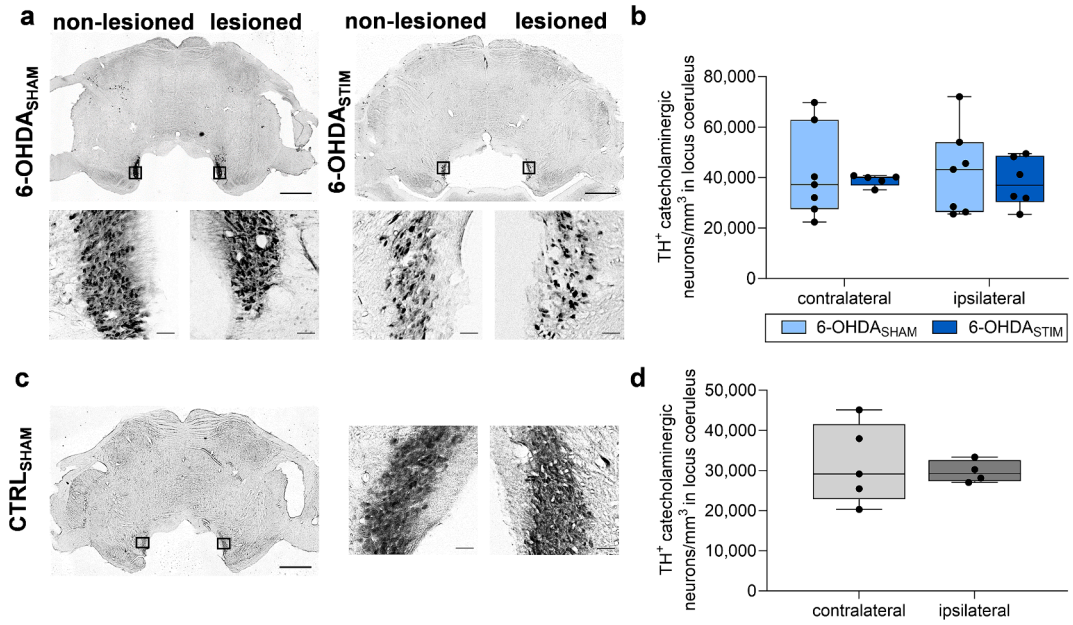

Fig. 4. Effects of six weeks of subthalamic nucleus deep brain stimulation (STN-DBS) on catecholaminergic cell counts in unilaterally 6-OHDA-lesioned rats (a) Representative images of TH staining in the *locus coeruleus* (LC) of hemiparkinsonian rats with either unilateral, right-sided STN-DBS for six weeks (6-OHDA$_{STIM}$) or sham stimulation (6-OHDA$_{SHAM}$). Scale bars, 1000 μm and 50 μm. **(b)** Quantitative analysis of TH$^+$ norepinephrenic neurons in the LC, 6-OHDA$_{SHAM}$ and 6-OHDA$_{STIM}$ animals showed no main effect of either 6-OHDA-lesioning or STN-DBS. **(c)** Representative immunohistological images of TH staining in the LC in healthy control rats. Scale bars, 1000 μm and 50 μm. **(d)** Quantification of TH$^+$ norepinephrinergic neurons in the LC showed no effect of electrode placement. *P*-values are from mixed ANOVA with Fisher LSD *post-hoc* analysis or unpaired, two-sided *t*-test as appropriate. Abbreviations: STN – nucleus subthalamicus; DBS – deep brain stimulation; 6-OHDA – 6-hydroxydopamine; LC – *locus coeruleus*; SHAM – sham stimulation; STIM – verum stimulation; TH – tyrosine hydroxylase; CTRL – healthy control rats.

parameters due to technical limitations (Fauser et al., 2021). Since we used amphetamine-induced rotations as compared to apomorphine treatment in the present cohort, the degree of DAergic deficiency is also not comparable to those in our previous studies, a factor which is discussed as an important issue for the neuroprotective and/or neurorestorative potential of STN-DBS (Maesawa et al., 2004, Spieles-Engemann et al., 2010, Fauser et al., 2021). However, the results on DA levels in the striatum with no effects of one week of STN-DBS are consistent with our previous findings that even though the DAergic neuron counts in the SNpc were slightly increased by STN-DBS, DAergic terminal densities in the STRd and NACC were unaltered by STN-DBS after one week of stimulation (Helf et al., 2023).

Our study is limited regarding its small cohorts due to the very high experimental effort in preclinical DBS studies; yet, the final group sizes are in line with similar studies (Spieles-Engemann et al., 2011, Fischer et al., 2017, Musacchio et al., 2017). We tried to minimize this limitation by using closely matched groups according to their quantitative apomorphine-induced rotational behaviour. In addition, the time interval between 6-OHDA lesioning and DBS onset was not exactly the same between cohorts (see Fig. 1 for details), which should however not influence our results according to the literature (Spieles-Engemann et al., 2010). Regarding the extent of dopaminergic degeneration, our previous cohort (cohort 2, (Helf et al., 2023)) presented with higher apomorphine-induced rotational scores and therefore possibly a higher degree of dopaminergic degeneration. Unfortunately, we used different histological methods to quantify TH$^+$ cell numbers, so these results are not comparable, while at the same time, the literature also questions the strong correlation between apomorphine-induced rotations and dopaminergic degeneration (Carman et al., 1991, Heuer et al., 2012). However, statistical analyses were only carried out within each cohort, i.e. between groups with identical and simultaneous treatment regimens. While high performance liquid chromatography with electrochemical detection (HPLC-ECD) is still considered the gold standard for measuring catecholamine levels and provides low detection levels (~1.5 ng of catecholamines per ml), it is also associated with comparatively high costs and requires experienced operators (Xie et al., 2018). On the other hand, catecholamine immunoassays are also an established method and have been implemented to analyse brain tissue homogenates (Muthuraju et al., 2015, Blazevic et al., 2020, Gong et al., 2020, Yang et al., 2022), however with higher detection levels, but significantly lower costs. In addition, we only included male animals, which limits the generalizability of our results, especially since both structural and functional differences in the LC-NE system between male and female rats have been reported (Curtis et al., 2006, Bangasser et al., 2011). In addition, NE levels might have been influenced by the type of neurostimulator, since the initial cohorts were treated with external backpack-worn stimulators, while the last cohort was fully implanted for long-term DBS to reduced animal strain (Plocksties et al., 2021). In translational terms, the 6-OHDA model – though it has been characterized extensively over several decades (Ungerstedt, 1968) – does not adequately reflect the neuropathological and clinical hallmarks of human PD, e.g. regarding α-synuclein accumulation and a chronic progressive course of the disease (Braak et al., 2003). This might limit the translational value of our results. However, even rodent models of α-synucleinopathies do not present with a similar degree of midbrain dopaminergic degeneration as compared to PD patients (Kordower et al., 2013, Nuber et al., 2013, Polissidis et al., 2021).

5. Conclusions

Our study provides first evidence that STN-DBS decreases striatal norepinephrinergic neurotransmission on the functional level. These findings could help to understand the mechanisms behind effects of STN-DBS on certain non-motor symptoms in PD patients. However, additional studies are clearly warranted to investigate the mechanistic involvement of NEergic neurotransmission in STN-DBS provoked non-motor symptoms.

Funding

This work was supported by the Deutsche Forschungsgemeinschaft (DFG) through the Collaborative Research Centre CRC 1270 "Electrically Active Implants" (DFG; SFB 1270/1,2 – 299150580) to all authors; M.F. was supported by the CRC 1270 "Electrically Active Implants" (DFG; SFB 1270/1 – 299150580) through the rotation position program for clinician scientists, by the Else Hirschberg Womeńs Advancement Program of the University Medical Centre Rostock and a research grant of the Deutsche Parkinsongesellschaft. F.S. was supported by the CRC 1270 "Electrically Active Implants" (DFG; SFB 1270/2 – 299150580) through an Integrated Research Training Program fellowship.

CRediT authorship contribution statement

Meike Statz: Writing – original draft, Methodology, Investigation, Formal analysis. **Hanna Weber:** Writing – review & editing, Investigation, Formal analysis. **Frederike Weis:** Investigation, Formal analysis. **Maria Kober:** Resources, Methodology, Investigation. **Henning Bathel:** Writing – review & editing, Software, Resources, Methodology. **Franz Plocksties:** Writing – review & editing, Software, Methodology. **Ursula van Rienen:** Writing – review & editing, Supervision, Funding acquisition. **Dirk Timmermann:** Writing – review & editing, Supervision, Funding acquisition. **Alexander Storch:** Writing – review & editing, Supervision, Funding acquisition, Conceptualization. **Mareike Fauser:** Writing – original draft, Funding acquisition, Conceptualization.

Declaration of Competing Interest

The authors declare that they have no known competing financial interests or personal relationships that could have appeared to influence the work reported in this paper.

Data availability

The datasets used and/or analysed during the current study are available from the corresponding author on reasonable request.

Acknowledgements

We gratefully acknowledge the help from Uta Naumann and Arian Eylmann with immunohistochemistry.

Appendix A. Supplementary data

Supplementary data to this article can be found online at https://doi.org/10.1016/j.brainres.2024.149128.

References

Albares, M., Thobois, S., Favre, E., Broussolle, E., Polo, G., Domenech, P., Boulinguez, P., Ballanger, B., 2015. Interaction of noradrenergic pharmacological manipulation and subthalamic stimulation on movement initiation control in Parkinson's disease. Brain Stimul. 8 (1), 27–35.

Alosaimi, F., Boonstra, J.T., Tan, S., Temel, Y., Jahanshahi, A., 2022. The role of neurotransmitter systems in mediating deep brain stimulation effects in Parkinson's disease. Front. Neurosci. 16, 998932.

Badstuebner, K., Gimsa, U., Weber, I., Tuchscherer, A., Gimsa, J., 2017. Deep brain stimulation of hemiparkinsonian rats with unipolar and bipolar electrodes for up to 6 weeks: behavioral testing of freely moving animals. Parkinsons Dis. 2017, 5693589.

Bangasser, D.A., Zhang, X., Garachh, V., Hanhauser, E., Valentino, R.J., 2011. Sexual dimorphism in locus coeruleus dendritic morphology: a structural basis for sex differences in emotional arousal. Physiol. Behav. 103 (3–4), 342–351.

Belujon, P., Bezard, E., Taupignon, A., Bioulac, B., Benazzouz, A., 2007. Noradrenergic modulation of subthalamic nucleus activity: behavioral and electrophysiological evidence in intact and 6-hydroxydopamine-lesioned rats. J. Neurosci. 27 (36), 9595–9606.

Betts, M.J., Kirilina, E., Otaduy, M.C.G., Ivanov, D., Acosta-Cabronero, J., Callaghan, M. F., Lambert, C., Cardenas-Blanco, A., Pine, K., Passamonti, L., Loane, C., Keuken, M. C., Trujillo, P., Lüsebrink, F., Mattern, H., Liu, K.Y., Priovoulos, N., Fliessbach, K., Dahl, M.J., Maaß, A., Madelung, C.F., Meder, D., Ehrenberg, A.J., Speck, O., Weiskopf, N., Dolan, R., Inglis, B., Tosun, D., Morawski, M., Zucca, F.A., Siebner, H. R., Mather, M., Uludag, K., Heinsen, H., Poser, B.A., Howard, R., Zecca, L., Rowe, J. B., Grinberg, L.T., Jacobs, H.I.L., Düzel, E., Hämmerer, D., 2019. Locus coeruleus imaging as a biomarker for noradrenergic dysfunction in neurodegenerative diseases. Brain 142 (9), 2558–2571.

Blazevic, S.A., Glogoski, M., Nikolic, B., Hews, D.K., Lisicic, D., Hranilovic, D., 2020. Differences in cautiousness between mainland and island Podarcis siculus populations are paralleled by differences in brain noradrenaline/adrenaline concentrations. Physiol. Behav. 224, 113072.

Braak, H., Del Tredici, K., Rub, U., de Vos, R.A., Jansen Steur, E.N., Braak, E., 2003. Staging of brain pathology related to sporadic Parkinson's disease. Neurobiol. Aging 24 (2), 197–211.

Brandt, M.D., Krüger-Gerlach, D., Hermann, A., Meyer, A.K., Kim, K.S., Storch, A., 2017. Early postnatal but not late adult neurogenesis is impaired in the Pitx3-mutant animal model of Parkinson's disease. Front. Neurosci. 11, 471.

Carman, L.S., Gage, F.H., Shults, C.W., 1991. Partial lesion of the substantia nigra: relation between extent of lesion and rotational behavior. Brain Res. 553 (2), 275–283.

Coenen, V.A., Gielen, F.L., Castro-Prado, F., Abdel Rahman, A., Honey, C.R., 2008. Noradrenergic modulation of subthalamic nucleus activity in human: metoprolol reduces spiking activity in microelectrode recordings during deep brain stimulation surgery for Parkinson's disease. Acta Neurochir. (Wien) 150 (8), 757–762 discussion 762.

Curtis, A.L., Bethea, T., Valentino, R.J., 2006. Sexually dimorphic responses of the brain norepinephrine system to stress and corticotropin-releasing factor. Neuropsychopharmacology 31 (3), 544–554.

Dafsari, H.S., Reddy, P., Herchenbach, C., Wawro, S., Petry-Schmelzer, J.N., Visser-Vandewalle, V., Rizos, A., Silverdale, M., Ashkan, K., Samuel, M., Evans, J., Huber, C.A., Fink, G.R., Antonini, A., Chaudhuri, K.R., Martinez-Martin, P., Timmermann, L., I. N.-M. S. S. Group, 2016. Beneficial effects of bilateral subthalamic stimulation on non-motor symptoms in Parkinson's disease. Brain Stimul. 9 (1), 78–85.

Dafsari, H.S., Silverdale, M., Strack, M., Rizos, A., Ashkan, K., Mahlstedt, P., Sachse, L., Steffen, J., Dembek, T.A., Visser-Vandewalle, V., Evans, J., Antonini, A., Martinez-Martin, P., Ray-Chaudhuri, K., Timmermann, L., E. a. t. I. N. M. P. S. Group, 2018. Nonmotor symptoms evolution during 24 months of bilateral subthalamic stimulation in Parkinson's disease. Mov. Disord. 33 (3), 421–430.

Delaville, C., Deurwaerdère, P.D., Benazzouz, A., 2011. Noradrenaline and Parkinson's disease. Front. Syst. Neurosci. 5, 31.

Deuschl, G., Paschen, S., Witt, K., 2013. Clinical outcome of deep brain stimulation for Parkinson's disease. Handb. Clin. Neurol. 116, 107–128.

Emmi, A., Campagnolo, M., Stocco, E., Carecchio, M., Macchi, V., Antonini, A., De Caro, R., Porzionato, A., 2023. Neurotransmitter and receptor systems in the subthalamic nucleus. Brain Struct. Funct. 228 (7), 1595–1617.

Ewing, S.G., Lipski, W.J., Grace, A.A., Winter, C., 2013. An inexpensive, charge-balanced rodent deep brain stimulation device: a step-by-step guide to its procurement and construction. J. Neurosci. Methods 219 (2), 324–330.

Faggiani, E., Delaville, C., Benazzouz, A., 2015. The combined depletion of monoamines alters the effectiveness of subthalamic deep brain stimulation. Neurobiol. Dis. 82, 342–348.

Fauser, M., Ricken, M., Markert, F., Weis, N., Schmitt, O., Gimsa, J., Winter, C., Badstubner-Meeske, K., Storch, A., 2021. Subthalamic nucleus deep brain stimulation induces sustained neurorestoration in the mesolimbic dopaminergic system in a Parkinson's disease model. Neurobiol. Dis. 156, 105404.

Fischer, D.L., Manfredsson, F.P., Kemp, C.J., Cole-Strauss, A., Lipton, J.W., Duffy, M.F., Polinski, N.K., Steece-Collier, K., Collier, T.J., Gombash, S.E., Buhlinger, D.J., Sortwell, C.E., 2017. Subthalamic nucleus deep brain stimulation does not modify the functional deficits or axonopathy induced by nigrostriatal α-synuclein overexpression. Sci. Rep. 7 (1), 16356.

Funkiewiez, A., Ardouin, C., Krack, P., Fraix, V., Van Blercom, N., Xie, J., Moro, E., Benabid, A.L., Pollak, P., 2003. Acute psychotropic effects of bilateral subthalamic nucleus stimulation and levodopa in Parkinson's disease. Mov. Disord. 18 (5), 524–530.

Gong, S.Q., Ye, T.T., Wang, M.X., Hong, Z.P., Liu, L., Chen, H., Qian, J., 2020. Profiling the mid-adult cecal microbiota associated with host healthy by using herbal formula Kang ShuaiLao Pian treated mid-adult mice. Chin. J. Nat. Med. 18 (2), 90–102.

Guimarães, J., Moura, E., Silva, E., Aguiar, P., Garrett, C., Vieira-Coelho, M.A., 2013. Locus coeruleus is involved in weight loss in a rat model of Parkinson's disease: an effect reversed by deep brain stimulation. Brain Stimul. 6 (6), 845–855.

Helf, C., Kober, M., Markert, F., Lanto, J., Overhoff, L., Badstübner-Meeske, K., Storch, A., Fauser, M., 2023. Subthalamic nucleus deep brain stimulation induces nigrostriatal dopaminergic plasticity in a stable rat model of Parkinson's disease. Neuroreport 34 (10), 506–511.

Heuer, A., Smith, G.A., Lelos, M.J., Lane, E.L., Dunnett, S.B., 2012. Unilateral nigrostriatal 6-hydroxydopamine lesions in mice I: motor impairments identify extent of dopamine depletion at three different lesion sites. Behav. Brain Res. 228 (1), 30–43.

Hezemans, F.H., Wolpe, N., O'Callaghan, C., Ye, R., Rua, C., Jones, P.S., Murley, A.G., Holland, N., Regenthal, R., Tsvetanov, K.A., Barker, R.A., Williams-Gray, C.H., Robbins, T.W., Passamonti, L., Rowe, J.B., 2022. Noradrenergic deficits contribute to apathy in Parkinson's disease through the precision of expected outcomes. PLoS Comput. Biol. 18 (5), e1010079.

Holland, N., Robbins, T.W., Rowe, J.B., 2021. The role of noradrenaline in cognition and cognitive disorders. Brain 144 (8), 2243–2256.

Kordower, J.H., Olanow, C.W., Dodiya, H.B., Chu, Y., Beach, T.G., Adler, C.H., Halliday, G.M., Bartus, R.T., 2013. Disease duration and the integrity of the nigrostriatal system in Parkinson's disease. Brain 136 (Pt 8), 2419–2431.
Krohn, F., Lancini, E., Ludwig, M., Leiman, M., Guruprasath, G., Haag, L., Panczyszyn, J., Düzel, E., Hämmerer, D., Betts, M., 2023. Noradrenergic neuromodulation in ageing and disease. Neurosci. Biobehav. Rev. 152, 105311.
Laurencin, C., Lancelot, S., Brosse, S., Mérida, I., Redouté, J., Greusard, E., Lamberet, L., Liotier, V., Le Bars, D., Costes, N., Thobois, S., Boulinguez, P., Ballanger, B., 2023. Noradrenergic alterations in Parkinson's disease: a combined 11C-yohimbine PET/neuromelanin MRI study. Brain.
Madelung, C.F., Meder, D., Fuglsang, S.A., Marques, M.M., Boer, V.O., Madsen, K.H., Petersen, E.T., Hejl, A.M., Løkkegaard, A., Siebner, H.R., 2022. Locus Coeruleus shows a spatial pattern of structural disintegration in Parkinson's disease. Mov. Disord. 37 (3), 479–489.
Maesawa, S., Kaneoke, Y., Kajita, Y., Usui, N., Misawa, N., Nakayama, A., Yoshida, J., 2004. Long-term stimulation of the subthalamic nucleus in hemiparkinsonian rats: neuroprotection of dopaminergic neurons. J. Neurosurg. 100 (4), 679–687.
Marsh, L., Biglan, K., Gerstenhaber, M., Williams, J.R., 2009. Atomoxetine for the treatment of executive dysfunction in Parkinson's disease: a pilot open-label study. Mov. Disord. 24 (2), 277–282.
Musacchio, T., Rebenstorff, M., Fluri, F., Brotchie, J.M., Volkmann, J., Koprich, J.B., Ip, C.W., 2017. Subthalamic nucleus deep brain stimulation is neuroprotective in the A53T alpha-synuclein Parkinson's disease rat model. Ann. Neurol. 81 (6), 825–836.
Muthuraju, S., Islam, M.R., Pati, S., Jaafar, H., Abdullah, J.M., Yusoff, K.M., 2015. Normobaric hyperoxia treatment prevents early alteration in dopamine level in mice striatum after fluid percussion injury: a biochemical approach. Int. J. Neurosci. 125 (9), 686–692.
Nomura, S., Bouhadana, M., Morel, C., Faure, P., Cauli, B., Lambolez, B., Hepp, R., 2014. Noradrenalin and dopamine receptors both control cAMP-PKA signaling throughout the cerebral cortex. Front. Cell. Neurosci. 8, 247.
Nuber, S., Harmuth, F., Kohl, Z., Adame, A., Trejo, M., Schönig, K., Zimmermann, F., Bauer, C., Casadei, N., Giel, C., Calaminus, C., Pichler, B.J., Jensen, P.H., Müller, C. P., Amato, D., Kornhuber, J., Teismann, P., Yamakado, H., Takahashi, R., Winkler, J., Masliah, E., Riess, O., 2013. A progressive dopaminergic phenotype associated with neurotoxic conversion of α-synuclein in BAC-transgenic rats. Brain 136 (Pt 2), 412–432.
Ohtsuka, C., Sasaki, M., Konno, K., Koide, M., Kato, K., Takahashi, J., Takahashi, S., Kudo, K., Yamashita, F., Terayama, Y., 2013. Changes in substantia nigra and locus coeruleus in patients with early-stage Parkinson's disease using neuromelanin-sensitive MR imaging. Neurosci. Lett. 541, 93–98.
Ostock, C.Y., Lindenbach, D., Goldenberg, A.A., Kampton, E., Bishop, C., 2014. Effects of noradrenergic denervation by anti-DBH-saporin on behavioral responsivity to L-DOPA in the hemi-parkinsonian rat. Behav. Brain Res. 270, 75–85.
Paredes-Rodriguez, E., Vegas-Suarez, S., Morera-Herreras, T., De Deurwaerdere, P., Miguelez, C., 2020. The noradrenergic system in Parkinson's Disease. Front. Pharmacol. 11, 435.
Pavese, N., Rivero-Bosch, M., Lewis, S.J., Whone, A.L., Brooks, D.J., 2011. Progression of monoaminergic dysfunction in Parkinson's disease: a longitudinal 18F-dopa PET study. Neuroimage 56 (3), 1463–1468.
Paxinos, G., Watson, C., 2007. The Rat Brain in Stereotaxic Coordinates. Academic Press, Amsterdam.
Plocksties, F., Kober, M., Niemann, C., Heller, J., Fauser, M., Nüssel, M., Uster, F., Franz, D., Zwar, M., Lüttig, A., Kröger, J., Harloff, J., Schulz, A., Richter, A., Köhling, R., Timmermann, D., Storch, A., 2021. The software defined implantable modular platform (STELLA) for preclinical deep brain stimulation research in rodents. J. Neural Eng. 18 (5).
Polissidis, A., Koronaiou, M., Kollia, V., Koronaiou, E., Nakos-Bimpos, M., Bogiongko, M., Vrettou, S., Karali, K., Casadei, N., Riess, O., Sardi, S.P., Xilouri, M., Stefanis, L., 2021. Psychosis-like behavior and hyperdopaminergic dysregulation in human α-Synuclein BAC transgenic rats. Mov. Disord. 36 (3), 716–728.
Schmitt, O., Eipert, P., 2012. neuroVIISAS: approaching multiscale simulation of the rat connectome. Neuroinformatics 10 (3), 243–267.
Schmitt, O., Eipert, P., Kettlitz, R., Leßmann, F., Wree, A., 2016. The connectome of the basal ganglia. Brain Struct. Funct. 221 (2), 753–814.
Spieles-Engemann, A.L., Behbehani, M.M., Collier, T.J., Wohlgenant, S.L., Steece-Collier, K., Paumier, K., Daley, B.F., Gombash, S., Madhavan, L., Mandybur, G.T., Lipton, J.W., Terpstra, B.T., Sortwell, C.E., 2010. Stimulation of the rat subthalamic nucleus is neuroprotective following significant nigral dopamine neuron loss. Neurobiol. Dis. 39 (1), 105–115.
Spieles-Engemann, A.L., Steece-Collier, K., Behbehani, M.M., Collier, T.J., Wohlgenant, S.L., Kemp, C.J., Cole-Strauss, A., Levine, N.D., Gombash, S.E., Thompson, V.B., Lipton, J.W., Sortwell, C.E., 2011. Subthalamic nucleus stimulation increases brain derived neurotrophic factor in the nigrostriatal system and primary motor cortex. J. Parkinsons Dis. 1 (1), 123–136.
Statz, M., Schleuter, F., Weber, H., Kober, M., Plocksties, F., Timmermann, D., Storch, A., Fauser, M., 2023. Subthalamic nucleus deep brain stimulation does not alter growth factor expression in a rat model of stable dopaminergic deficiency. Neurosci. Lett. 814, 137459.
Temel, Y., Visser-Vandewalle, V., Kaplan, S., Kozan, R., Daemen, M.A., Blokland, A., Schmitz, C., Steinbusch, H.W., 2006. Protection of nigral cell death by bilateral subthalamic nucleus stimulation. Brain Res. 1120 (1), 100–105.
Ungerstedt, U., 1968. 6-Hydroxy-dopamine induced degeneration of central monoamine neurons. Eur. J. Pharmacol. 5 (1), 107–110.
Volkmann, J., Herzog, J., Kopper, F., Deuschl, G., 2002. Introduction to the programming of deep brain stimulators. Mov. Disord. 17 (Suppl 3), S181–S187.
Waddington, J.L., 1980. Effects of nomifensine and desipramine on the sequelae of intracerebrally-injected 6-OHDA and 5,6-DHT. Pharmacol. Biochem. Behav 13 (6), 915–917.
Wang, Y., Zhang, Q.J., Liu, J., Ali, U., Gui, Z.H., Hui, Y.P., Wang, T., Chen, L., Li, Q., 2010. Noradrenergic lesion of the locus coeruleus increases the firing activity of the medial prefrontal cortex pyramidal neurons and the role of alpha2-adrenoceptors in normal and medial forebrain bundle lesioned rats. Brain Res. 1324, 64–74.
Weselek, G., Keiner, S., Fauser, M., Wagenführ, L., Müller, J., Kaltschmidt, B., Brandt, M. D., Gerlach, M., Redecker, C., Hermann, A., Storch, A., 2020. Norepinephrine is a negative regulator of the adult periventricular neural stem cell niche. Stem Cells.
Xie, L., Chen, L., Gu, P., Wei, L., Kang, X., 2018. A convenient method for extraction and analysis with high-pressure liquid chromatography of catecholamine neurotransmitters and their metabolites. J. Vis. Exp. 133.
Yang, X., Liu, W., Dang, P., Wang, Y., Ge, X., Huang, X., Wang, M., Zheng, J., Ding, X., Wang, X., 2022. Decreased brain noradrenaline in minimal hepatic encephalopathy is associated with cognitive impairment in rats. Brain Res. 1793, 148041.
Zarow, C., Lyness, S.A., Mortimer, J.A., Chui, H.C., 2003. Neuronal loss is greater in the locus coeruleus than nucleus basalis and substantia nigra in Alzheimer and Parkinson diseases. Arch. Neurol. 60 (3), 337–341.
Zweig, R.M., Cardillo, J.E., Cohen, M., Giere, S., Hedreen, J.C., 1993. The locus ceruleus and dementia in Parkinson's disease. Neurology 43 (5), 986–991.